Brawerman, G. (1988) *Cell 57*, 9-10.
Brewer, G., & Ross, J. (1988) *Mol. Cell. Biol. 8*, 1697-1708.
Brown, B. D., & Harland, R. M. (1990) *Genes Dev. 4*, 1925-1935.
Cleveland, D. W., & Yen, T. J. (1989) *New Biol. 1*, 121-126.
Cochrane, A., & Deeley, R. G. (1989) *J. Biol. Chem. 264*, 6495-6503.
Kazmaier, M., Bruning, E., & Ryffel, G. U. (1985) *EMBO J. 4*, 1261-1266.
Moskaitis, J. E., Pastori, R. L., & Schoenberg, D. R. (1990) *Nucleic Acids Res. 18*, 2184.
Moskaitis, J. E., Buzek, S. W., Pastori, R. L., & Schoenberg, D. R. (1991) *Biochem. Biophys. Res. Commun. 174*, 825-830.
Nielsen, D. A., & Shapiro, D. J. (1990) *Mol. Endocrinol. 4*, 953-957.
Pachter, J. S., Yen, T. J., & Cleveland, D. W. (1987) *Cell 48*, 599-605.
Pastori, R. L., Moskaitis, J. E., Smith, L. H., & Schoenberg, D. R. (1990) *Biochemistry 29*, 2599-2605.
Pastori, R. L., Moskaitis, J. E., Buzek, S. W., & Schoenberg, D. R. (1991) *Mol. Endocrinol. 4*, 461-468.
Pei, R., & Calame, K. (1988) *Mol. Cell. Biol. 8*, 2860-2868.
Rao, T. R., & Slobin, L. I. (1988) *Mol. Cell. Biol. 8*, 1085-1092.
Riegel, A. T., Martin, M. B., & Schoenberg, D. R. (1986) *Mol. Cell. Endocrinol. 44*, 201-209.
Ross, J., Peltz, S. W., Kobs, G., & Brewer, G. (1986) *Mol. Cell. Biol. 6*, 4362-4371.
Ross, J., Kobs, G., Brewer, G., Peltz, S. W. (1987) *J. Biol. Chem. 262*, 9374-9381.
Schoenberg, D. R., Moskaitis, J. E., Smith, L. H., & Pastori, R. L. (1989) *Mol. Endocrinol. 3*, 805-814.
Shaw, G., & Kamen, R. (1986) *Cell 46*, 659-667.
Shyu, A. B., Greenberg, M. E., & Belasco, J. G. (1989) *Genes Dev. 3*, 60-72.
Wilson, T., & Treisman, R. (1988) *Nature 336*, 396-399.
Wolffe, A. P., Glover, J. F., Martin, S. C., Tenniswood, M. P. R., Williams, J. L., & Tata, J. R. (1985) *Eur. J. Biochem. 146*, 489-496.
Yen, T. J., Machlin, P. S., & Cleveland, D. W. (1988) *Nature 334*, 580-585.
Zelus, B. D., Giebelhaus, D. H., Eib, D. W., Kenner, K. A., & Moon, R. T. (1989) *Mol. Cell. Biol. 9*, 2756-2760.

Analysis of the RNA- and DNA-Dependent DNA Polymerase Activities of Point Mutants of HIV-1 Reverse Transcriptase Lacking Ribonuclease H Activity†

Lindsay R. Dudding, N. Cyril Nkabinde, and Valerie Mizrahi*

Molecular Biology Unit of the South African Institute for Medical Research and Department of Haematology, University of the Witwatersrand Medical School, P.O. Box 1038, Johannesburg 2000, South Africa

Received May 7, 1991; Revised Manuscript Received July 29, 1991

ABSTRACT: The RNA- and DNA-dependent DNA polymerase activities of two point mutants of HIV-1 reverse transcriptase lacking ribonuclease H activity have been compared to the wild-type enzyme activities using substrates consisting of an oligodeoxynucleotide primer hybridized to either a RNA or a DNA template. The RNase H phenotype had a negligible effect on the steady-state kinetics and processivity of reverse transcription of a homopolymer template-primer [poly(A)·oligo(dT)]. However, analysis of the distribution of DNA products indicated that the ability of the mutants to reverse-transcribe a specifically primed 345-nucleotide heteropolymeric RNA template derived from the *gag* region of HIV-1 was impaired relative to the wild-type enzyme. Although the wild-type and mutant enzymes shared the same pause sites of synthesis along the RNA template, certain prematurely terminated nascent primer chains were poorly extended by the mutant enzymes and hence accumulated, suggesting that a catalytically functional RNase domain facilitated reinitiation of DNA synthesis at specific pause sites along a heteropolymer template. In contrast, the processivity and product distribution of DNA synthesis directed by a heteropolymer *gag* DNA template of the same nucleotide sequence were not significantly influenced by the RNase H phenotype of the mutants.

In the search for novel therapeutic strategies against acquired immune deficiency syndrome (AIDS),[1] the enzymes encoded by the causative agent, HIV-1, are under intense scrutiny as potential targets for rational drug design. The reverse transcriptase (RT) enzyme encoded by a retrovirus is solely responsible for converting the ss-RNA genome into a ds-proviral DNA form, which is the substrate for integration of the virus into the genome of the infected host cell (Panganiban & Fiore, 1988). The three RT-associated activities needed to accomplish this task are (i) RNA-dependent DNA polymerase, (ii) ribonuclease H, and (iii) DNA-dependent DNA polymerase (Goff, 1990). The experimental data bearing on the structure–function relationships in HIV-1 RT were recently reviewed by Jacobo-Molina and Arnold (1991). The linker insertion mutagenesis data of Prasad and Goff (1989) and of Hizi et al. (1990), in conjunction with the identification of a carboxy-terminal "p15" RNase H activity (Hansen et al., 1988), suggested that the domain organization of HIV-1 RT parallels that of other RT enzymes, with the RNase H and polymerase domains distinct and separate from one another

† This research was funded by grants from the Foundation for Research and Development, the Medical Research Council of South Africa, and the South African Institute for Medical Research. Presented in part at the IUB 15th International Congress of Biochemistry, Jerusalem, 1991.

* Address correspondence to this author.

[1] Abbreviations: AIDS, acquired immune deficiency syndrome; HIV-1, human immunodeficiency virus type 1; RT, reverse transcriptase; RNase H; ribonuclease H; nt, nucleotide(s); ss, single stranded; ds, double stranded; dNTP, deoxynucleoside 5′-triphosphate; Tris·HCl, tris(hydroxymethyl)aminomethane hydrochloride; EDTA, ethylenediaminetetraacetic acid; DTT, dithiothreitol; SDS, sodium dodecyl sulfate.

0006-2960/91/0430-10498$02.50/0

(Kotewicz et al., 1988; Tanese & Goff, 1988). Further evidence in support of the modular domain organization was recently obtained from site-directed mutagenesis studies, in which the substitution of highly conserved acidic residues within the carboxy-terminal portion of the RT coding region specifically repressed RNase H function, without significantly affecting the RT activity of the enzyme (Schatz et al., 1989; Mizrahi et al., 1990). However, the combined mutagenesis data of this enzyme have suggested that although the activities may be physically separable (Hansen et al., 1988; Prasad & Goff, 1989), many mutations in one domain had a global effect on both activities rather than a purely local effect on one activity (Prasad & Goff, 1989; Hizi et al., 1990; Mizrahi et al., 1990), thereby implicating an interaction between the two functionally distinct (Davies et al., 1991; Hostomsky et al., 1991; Tan et al., 1991) and uncoupled (DeStefano et al., 1991) domains in the context of the p66/p51 heterodimer form of the enzyme.

We recently reported that the single and double aspartic acid to asparagine point mutants of HIV-1 RT, D443N and D443N/D498N, lacked detectable RNase H activity but appeared to retain wild-type levels of RT activity on a homopolymeric template-primer (Mizrahi et al., 1990). Since the specific RNase H phenotype conferred by these conservative mutations offered a useful probe for studying the functional interaction between the polymerase and ribonuclease activities, we further investigated their effects on the DNA polymerase activities of the enzyme using related heteropolymeric RNA and DNA templates, and report on the results of that study herein.

Materials and Methods

Materials

Sources of commercial enzymes, nucleotides, and radionucleotides were as previously described (Dudding et al., 1990). Recombinant HIV-1 RT enzymes (wild type, D443N, and D443N/D498N mutants) were purified as previously described (Mizrahi et al., 1989, 1990; Dudding et al., 1990). The relative concentrations of the RT enzymes in an SDS–polyacrylamide gel were measured by comparative densitometric quantitation of the p66 and p51 polypeptides. The T7 RNA polymerase expression system *Escherichia coli* BL21/pAR1219 was kindly provided by Prof. F. W. Studier. The enzyme was purified according to a modification of the procedure described by Grodberg and Dunn (1988), in which the ammonium sulfate precipitate was purified by chromatography over S-Sepharose Fast Flow (Sigma; batch-eluted with buffer C/200 mM NaCl), followed by CM-Sepharose Fast Flow (Sigma, batch-eluted with buffer C/200 mM NaCl) and Q-Sepharose Fast Flow (Sigma; eluted with a linear gradient of buffer C containing 25–440 mM NaCl). The transcription vector pGEM-ΔGAG-C used for the preparation of (+)-GAG^{345} RNA was previously described (Dudding et al., 1990). The 60-nt RNA (+)-GEM^{60}, prepared by runoff transcription of *Hin*dIII-digested pGEM-3Zf(+) (Promega) using T7 RNA polymerase, corresponded to the sequence of the multiple cloning site of the plasmid between the T7 transcriptional initiation site and the *Hin*dIII site. The oligonucleotide primers GAG-1 (5′-TTGCTCGGCTCTTAGAG-3′), GAG-2 (5′-GTCTACATAGTCTCTAAAA-3′), GAG-3 (5′-ATAGAACCGGTCTACATAG-3′), GAG-4 (5′-ACCGGTCTACATAGTCTC-3′), and GEM-1 (5′-AGCTTGCATGCCTGCAGGT-3′) were synthesized using a MilliGen/Biosearch Cyclone oligonucleotide synthesizer and were purified by Millipore Oligopak cartridge reverse-phase chromatography prior to use. The oligonucleotides dT_{12} and dT_{12-18} were purchased from Pharmacia, and poly(A) was from Boehringer-Mannheim. Oligonucleotide concentrations were estimated spectrophotometrically (A_{260} = 1 for 20 μg/mL). The *gag* primers were complementary to (+)-GAG^{345} between positions 326–342 (GAG-1), 294–312 (GAG-2), 303–321 (GAG-3), and 299–316 (GAG-4), where position 345 represents the 3′-terminal nt of the RNA. GEM-1 was complementary to (+)-GEM^{60} between positions 42 and 60, where position 60 represents the 3′-terminal nt of the RNA. The M13 subclone M13-ΔGAG-C was constructed by forced clockwise cloning of the 297 bp *Pst*I/*Hin*dIII fragment from pGEM-ΔGAG-C into M13mp18. Liquid scintillation counting was performed on a Beckman LS 6000IC counter using a Packard toluene scintillator. Densitometry was performed with a Biomed Inc. video camera densitometer.

Methods

Substrate Preparation. Oligonucleotides were 5′-^{32}P-end-labeled as previously described (Mizrahi et al., 1986). Unlabeled (+)-GAG^{345} and (+)-GEM^{60} were prepared by T7 RNA polymerase runoff transcription of *Hin*dIII-digested pGEM-ΔGAG-C or pGEM-3Zf(+). Reactions (40–250 μL) containing 40 mM Tris·HCl (pH 7.5), 12 mM $MgCl_2$, 2 mM spermidine, 10 mM DTT, 1 unit/μL RNase inhibitor, 250 μM each of ATP, CTP, GTP, and UTP, *Hin*dIII-digested pGEM-ΔGAG-C or pGEM-3Zf(+) (0.3 μg/μL), and T7 RNA polymerase (2 units/μL) were incubated at 39–40 °C for 2 h. Reactions were quenched by phenol/chloroform (1:1) extraction followed by ethanol precipitation. The RNA was gel-purified as previously described (Dudding et al., 1990). The eluent was concentrated and further purified by centrifugation through a Millipore Ultrafree-MC filter unit (10000 NMWL) in a Millipore Personal centrifuge (2000*g*, 15 min, 4 °C). The retentate was diluted with water (400 μL), and the RNA was obtained by ethanol precipitation in the presence of 0.3 M sodium acetate. The concentration of the purified RNA was estimated on the basis of a control synthesis and purification run in which the RNA was trace-labeled with [^{32}P]UMP of known specific activity. The RNA was stored in TE buffer [10 mM Tris·HCl (pH 8.0)/1 mM EDTA] at −70 °C at a concentration of 600 nM. Single-stranded DNA template complementary to the oligonucleotides GAG-1–GAG-4 was isolated from M13-ΔGAG-C phage supernatant as previously described (Mizrahi, 1989).

Hybridization. Mixtures containing 100–150 nM primer and either 300 nM ss-M13-ΔGAG-C DNA or 350–550 nM (+)-GAG^{345} RNA or (+)-GEM^{60} in hybridization buffer [40 mM Tris·HCl (pH 7.9), 40 mM KCl, and 4 mM $MgCl_2$] were placed in a wath bath initially at either 50 °C (RNA template) or 65 °C (DNA template) and allowed to cool to room temperature.

DNA Polymerase Assays. (1) Filter Assay. The standard DE81 filter assay for RT activity using a poly(A)·dT_{12-18} template-primer was based on that previously described (Mizrahi et al., 1989). For the steady-state kinetic study, a 50-μL aliquot of assay cocktail was mixed at 37 °C with 12.5 μL of RT enzyme [diluted in RT storage buffer (Mizrahi et al., 1989)] to give a final reaction containing 67 mM Tris·HCl (pH 7.9), 57 mM KCl, 20 mM NaCl, 6.9 mM $MgCl_2$, 0.2 mM EDTA, 2–200 nM poly(A)·dT_{12-18} ([3′-OH]; 20:1 A:T nucleotide ratio), 4 mM DTT, 0.02% Triton X-100, 10% glycerol, 40 μM [^{3}H]TTP (880–2640 dpm/pmol), and 0.5–2 nM RT enzyme, which was incubated at 37 °C. Aliquots (12 μL) were quenched after 0, 20, 40, 60, 90, 120, and 180 s with 15 μL of 0.1 M EDTA (pH 8.0) and were assayed by the

DE81 filter method (Mizrahi, 1989). The counting efficiency of ^3H in nucleic acid bound to DE81 was measured by comparing the incorporation data for parallel polymerization assays containing either [^{32}P]TTP or [^{3}H]TTP (880 dpm/pmol) under otherwise identical conditions. The efficiency was 24%. For the steady-state kinetic study using the ss-M13-ΔGAG-C/GAG-1 substrate, final reactions (60 μL) containing 57 mM Tris·HCl (pH 7.9), 57 mM KCl, 17 mM NaCl, 5.7 mM $MgCl_2$, 0.2 mM EDTA, 7–120 nM ss-M13-ΔGAG-C/GAG-1 ([3′-OH]; 3:1 template:primer molar ratio), 5 mM DTT, 0.02% Triton X-100, 8% glycerol, 42 μM dNTP (N = A, C, and G), 17 μM [α-^{32}P]TTP (5500 dpm/pmol), and 2–10 nM enzyme were incubated at 37 °C. Aliquots (12 μL) were quenched as above after 0, 0.5, 1, 2, 5, and 10 min and assayed by the DE81 filter method.

(*2*) *Gel Electrophoretic Assay*. Unless otherwise indicated, reactions (12 μL) containing 63 mM Tris·HCl (pH 7.9), 55 mM KCl, 16 mM NaCl, 0.2 mM EDTA, 8.3 mM $MgCl_2$, 0.02% Triton X-100, 8% glycerol, 5 mM DTT, 30 nM ^{32}P-labeled hybrid ([3′-OH]; ca. 2×10^6 dpm), and RT (15–170 nM) were incubated at 37 °C. Aliquots were withdrawn after 0.5–30 min and were quenched and electrophoresed in a 12–15% polyacrylamide/7 M urea gel as previously described (Mizrahi, 1989; Dudding et al., 1990). Gels were autoradiographed at −70 °C with an intensifier screen using 3M Trimax type XDA X-ray film. Autoradiographs were exposed to obtain band intensities within the linear response range of the film, as measured by densitometry of multiple exposures of a standard gel.

Processivity Assays. The DNA trap was prepared as described by Joyce (1989) using salmon sperm DNA. Processivity assays and controls were modeled after those described by Joyce (1989). Mixtures (6 μL) containing 20 nM hybrid, 4–100 nM RT enzyme, 17 mM Tris·HCl (pH 7.9), 17 mM KCl, 1.7 mM $MgCl_2$, and 2 mM EDTA were preincubated at 37 °C for 1 min. Reactions were initiated by vigorously mixing the E·hybrid solution with 6 μL of a solution containing 10 mg/mL trap DNA, 80 μM dNTPs, 110 mM Tris·HCl (pH 7.9), 110 mM KCl, 11 mM $MgCl_2$, and 2 mM DTT, to give a final reaction containing 10 nM hybrid, 2–50 nM enzyme, 5 mg/mL trap DNA, 40 μM dNTPs, 63 mM Tris·HCl, 63 mM KCl, 1 mM EDTA, 6.3 mM $MgCl_2$, and 1 mM DTT. Reactions were incubated at 37 °C, and 3-μL aliquots were quenched after 0–2 min and electrophoresed as described above. Unchallenged control reactions were conducted by omitting the DNA trap. Control experiments designed to test the efficacy of the trap were conducted by including the trap in the preincubation of RT with hybrid and initiating polymerization with Mg-dNTPs. Quenched samples were electrophoresed as above.

Computation. Secondary structural predictions (inverted repeats, folded forms) for the RNA templates (+)-GAG^{345} and (+)-GEM^{60} were made using the StemLoop and Squiggles modules of the GCG Version 5 Package (University of Wisconsin) on the VAX computer at the University of Cape Town. Michaelis–Menten kinetic parameters were computed by data analysis using Enzfitter Version 1.03 (Leatherbarrow, R. J., Elsevier Biosoft, 1987) on an IBM personal computer.

Results

RNA-Dependent DNA Synthesis. (*1*) *Homopolymer Template-Primer*. The results of a comparative steady-state kinetic analysis of the three enzymes using a poly(A)·dT_{12-18} homopolymer template-primer are summarized in Table I. The mutations were found to have a negligible effect on the kinetic parameters for reverse transcription of this substrate.

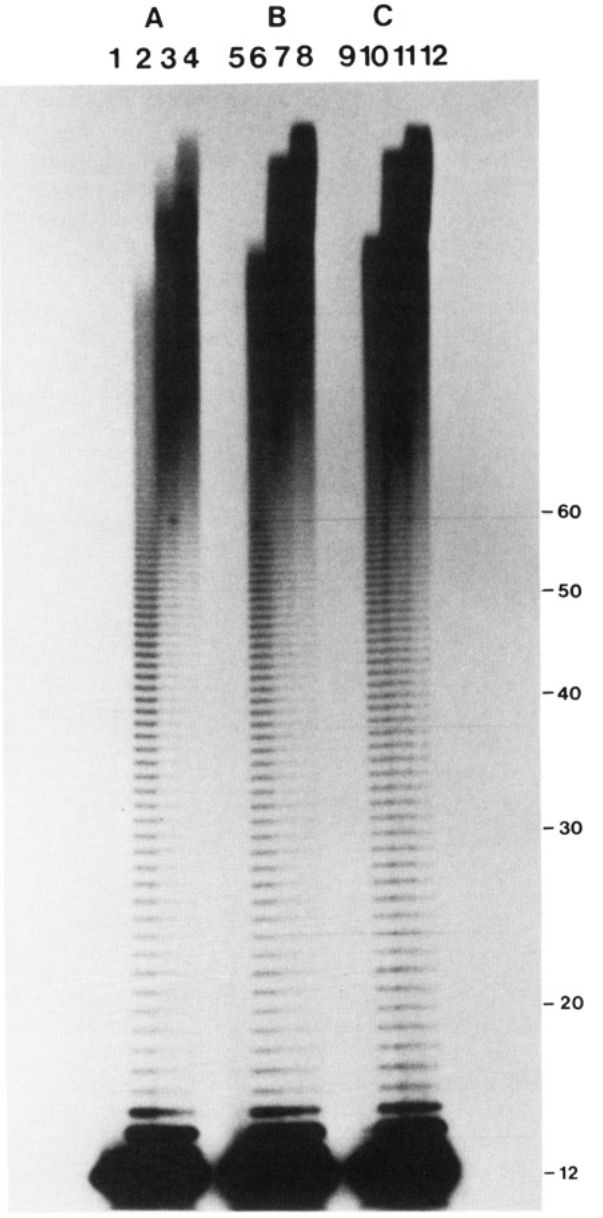

FIGURE 1: Homopolymer RNA-dependent DNA polymerization. Time courses of DNA synthesis of poly(A)·[5′-^{32}P]dT_{12} catalyzed by wild-type (panel A), D443N (panel B), and D443N/D498N (panel C) RT enzymes. Reactions (12 μL) were initiated by mixing 6 μL of a mixture containing 17 mM Tris·HCl (pH 7.9), 17 mM KCl, 1.7 mM $MgCl_2$, 2 mM EDTA, and 208 nM ^{32}P-labeled hybrid (expressed as [3′-OH]; 20:1 A:T nt ratio) with an equal volume of a mixture containing 111 mM Tris·HCl (pH 7.9), 111 mM KCl, 11 mM $MgCl_2$, 2 mM DTT, 83 μM TTP, and 21 nM enzyme. Final reactions containing 64 mM Tris·HCl, 64 mM KCl, 6.4 mM $MgCl_2$, 1 mM EDTA, 1 mM DTT, 41 μM TTP, 104 nM hybrid, and 10 nM enzyme were incubated at 37 °C. Aliquots (3 μL) were quenched with 3 μL of gel loading buffer after 0 (lanes 1, 5, and 9), 15 (lanes 2, 6, and 10), 30 (lanes 3, 7, and 11), and 45 s (lanes 4, 8, and 12), and were electrophoresed in a 15% polyacrylamide/7 M urea gel, as described under Materials and Methods. The product sizes are indicated.

The products of homopolymer synthesis were visualized by gel electrophoretic analysis of time courses using a poly(A)·[5′-^{32}P]dT_{12} substrate (Figure 1). The product distributions generated by the wild type (panel A) and D443N mutant (panel B) were very similar in all cases. In agreement with the observations of Majumdar et al. (1988), termination occurred with high frequency after the addition of the first 1–3 nt, beyond which further synthesis proceeded with high processivity to form large products (>70 nt). The slight skewing of the D443N/D498N product distribution in favor of products

Table I: Steady-State Kinetic Parameters of the Wild-Type and Mutant Enzymes for Reverse Transcription of a Homopolymer RNA·DNA Substrate[a]

enzyme	k_{cat} (s^{-1})[b]	K_M (nM)
wild type	4.0 ± 0.2	4.0 ± 1.0
D443N	3.7 ± 0.3	3.3 ± 1.5
D443N/D498N	3.7 ± 0.2	5.1 ± 1.5

[a] RT filter assays were performed as described under Materials and Methods. Rates were proportional to enzyme concentration over this substrate concentration range. At each substrate concentration, initial rates were measured in duplicate from 0–3-min time courses. [b] The concentration of total protein was used as an approximation of the active enzyme concentration.

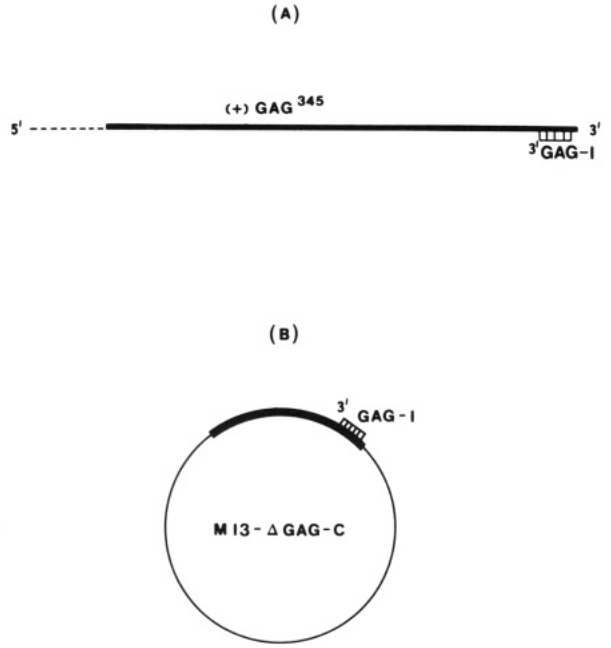

FIGURE 2: Structures of the heteropolymer *gag* hybrid substrates. The thick line in both panels represents the same 297-nt sequence between the *Pst*I and *Hin*dIII sites of the *gag* region of HIV-1 (Mizrahi, 1989). (Panel A) RNA·DNA hybrid structures showing the positions of complementarity between the oligonucleotide primer GAG-1 and the RNA transcript (+)-GAG^{345} (Dudding et al., 1990). The dashed region at the 5′ end of (+)-GAG^{345} corresponds to the transcribed sequence between the T7 RNA polymerase transcriptional initiation site and the *Pst*I junction with the 297 bp *gag* insert. (Panel B) DNA·DNA hybrid structures showing the position of complementarity between the GAG-1 oligonucleotide primer and the ss-DNA derived from the M13 subclone M13-ΔGAG-C.

of intermediate size (15–70 nt; panel C) suggested that the processivity of this mutant was marginally lower than that of the wild-type and D443N enzymes (lane 11 versus lanes 3 and 7).

(*2*) *Heteropolymer Template-Primer.* The structures of the heteropolymer *gag* hybrids used in this study are illustrated in Figure 2. The gel electrophoretic time courses for RNA-dependent DNA polymerization of the (+)-GAG^{345}/GAG-1 hybrid substrate catalyzed by equimolar amounts of the wild-type (panel A), D443N (panel B), and D443N/D498N (panel C) HIV-1 RT enzymes are illustrated in Figure 3. Although the time courses were qualitatively similar, the product distributions generated by the RNase H enzymes (panels B and C) differed quantitatively from that of the wild-type enzyme (panel A) with respect to the relative abundance of the pause-site products RI–RXV. Termination of the wild type at a major pause site located approximately 70 nt downstream of the 3′-terminus of the GAG-1 primer resulted in the accumulation of the RXII product(s), whereas

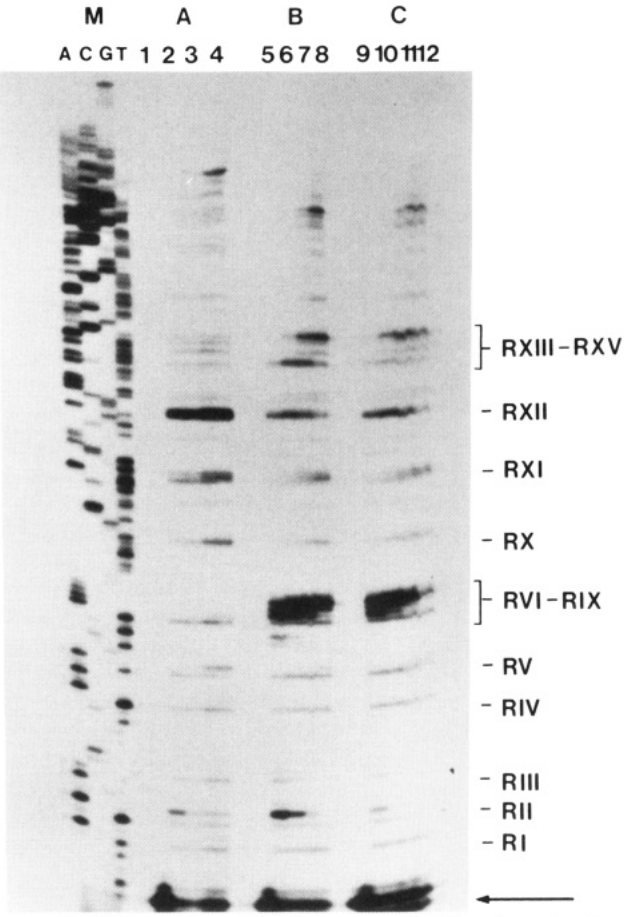

FIGURE 3: Heteropolymer RNA-dependent DNA polymerization. Time courses of RT-catalyzed DNA synthesis of (+)-GAG^{345}/[5′-^{32}P]GAG-1 substrate catalyzed by wild-type (panel A), D443N (panel B), and D443N/D498N (panel C) enzymes. Reactions containing 30 nM hybrid and 170 nM enzyme were incubated as described under Materials and Methods. Time points were quenched after 0 (lanes 1, 5, and 9), 2 (lanes 2, 6, and 10), 5 (lanes 3, 7, and 11), and 10 min (lanes 4, 8, and 12). The positions of the synthetic pause sites were determined by alignment against a sequencing ladder that was generated by dideoxy sequencing of ss-M13-ΔGAG-C with 5′-^{32}P-labeled GAG-1 primer (panel M; lanes A, C, G, and T). Samples were electrophoresed in a 12% polyacrylamide/7 M urea gel, as described under Materials and Methods. The position of the unextended GAG-1 primer is indicated by an arrow. The termination products RI–RXV are referred to in the text.

the mutants preferentially terminated 28–31 nt beyond the GAG-1 primer terminus to form the RVI–RIX products. The addition of a 5-fold excess of D443N enzyme to the product mixture of a 5-min incubation with D443N enzyme, under the conditions of Figure 3, lane 7 (final [E] = 800 nM), resulted in minimal further extension of the pause-site products, suggesting that these intermediates represented severe blocks to full-length cDNA synthesis by an RNase H$^-$ enzyme (data not shown). To test whether the difference in the wild-type versus mutant product distributions was simply due to a faster rate of synthesis by the wild-type enzyme, which would favor the formation of larger termination products by the further extension of smaller intermediates, the wild-type time course generated at a 10-fold lower enzyme concentration was analyzed. Although the overall extent of polymerization was reduced, the relative concentration of the RXII product(s) remained significantly higher than the RVI–RIX cluster, suggesting that the differences observed in Figure 3 indeed reflected a dependence of the specific termination frequencies at certain pause sites on the RNase H phenotype of the enzyme (data not shown).

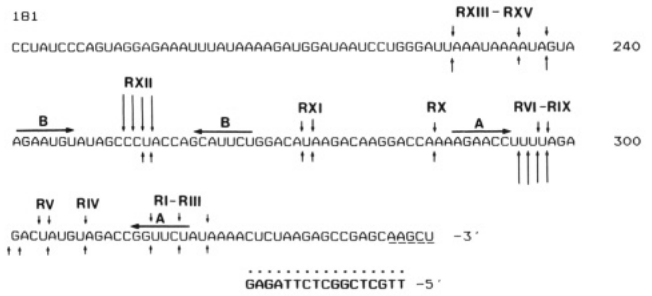

FIGURE 4: Pause sites of DNA synthesis along the *gag* RNA template. The locations of the pause sites RI–RXV (referred to in the text) within the 3′-terminal region of the (+)-GAG^{345} RNA template (bases 181–345) are indicated by the arrows *above* (wild type) or *below* (mutants) the corresponding template position. The arrow height indicates the relative concentration of the product formed under the multiple turnover conditions of Figure 3. The inverted repeat sequences giving rise to the putative stem loops A and B are indicated by horizontal arrows above the sequence. The position of complementarity of the GAG-1 primer to the RNA template is indicated.

The template positions and the relative concentrations of the pause-site products formed during the multiple enzyme turnover time courses of Figure 3 are illustrated in Figure 4. No obvious correlation between pause-site location and primary template sequence was found, in accordance with the observations of Huber et al. (1989). With respect to correlation with regions of RNA secondary structure, several inverted repeat sequences were identified within (+)-GAG^{345}. The major pause sites of both the wild-type (RXII) and mutant enzymes (RVI–RIX) were clustered within the loop regions of the hairpins formed by repeats B and A, respectively (Figure 4). The positions of the pause sites were unaffected by increasing the polymerization temperature to 42 °C (data not shown), arguing against a causative role of RNA secondary structure in determining the pause-site locations of HIV-1 RT, in agreement with the conclusions of Huber et al. (1989). However, it is possible that this temperature shift was not sufficiently high to totally disrupt the hairpins A and B, in which case secondary structural determinants could not be totally excluded.

To test whether the pause-site locations were influenced by distance from the initial 3′-terminus of the hybrid, the GAG-1 primer was replaced by GAG-2, which primed synthesis a further 32 nt downstream of the GAG-1 3′-terminus (i.e., 1 nt downstream of the RIX template position). In all cases, the locations of the preferred pause sites at positions RX–RXV and the relative concentrations of the corresponding products were unaffected by this 32-nt downstream move of the initial primer terminus. Furthermore, the preferential termination of the mutants relative to the wild type at positions RVI–RIX was maintained when GAG-1 was replaced by GAG-3, which primed synthesis 5 nt upstream of the RVI position (data not shown). However, when the initial primer terminus was located only 1 nt upstream of the RVI position (GAG-4), both the wild-type and mutant enzymes paused at the adjacent RVI–RIX sites with approximately equal frequency (data not shown).

To further explore the potential role of RNA secondary structure in pause-site determination, the products of reverse transcription of a second, unrelated heteropolymeric RNA template, (+)-GEM^{60}, were analyzed (data not shown). Once again, the mutants and the wild type shared the same pause sites of synthesis which were clustered within regions of potential stem–loop structure. Although the mutant versus wild-type time courses did not differ as noticeably as was observed for the *gag* template (Figure 3), the amount of

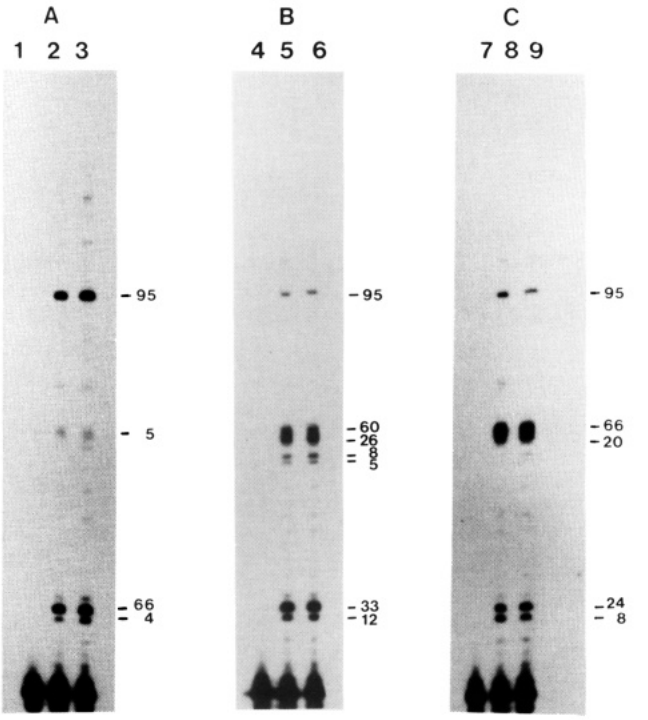

FIGURE 5: Processivity of DNA synthesis on an RNA heteropolymer template. (Panel A) Wild type; (panel B) D443N; (panel C) D443N/D498N. The hybrid substrate was (+)-GAG^{345}/[5′-^{32}P]-GAG-1. Lanes, 1, 4, and 7, control polymerization products formed when the trap was included in the preincubation of the enzyme and substrate. Lanes 3, 6, and 9, control polymerization products formed in the absence of trap. Lanes 2, 5, and 8, products of a single processive cycle. In all cases, final polymerization reactions containing 10 nM hybrid and 2 nM enzyme were incubated as described under Materials and Methods and were quenched after 1 min. Samples were electrophoresed on a 15% polyacrylamide/7 M urea gel. The numbers to the right of the panels represent the termination frequencies (in percent) of the enzymes at the indicated template positions during a single processive cycle of synthesis.

full-length product synthesized by the wild-type enzyme was markedly higher than that formed by the mutants, suggesting that the catalytically functional RNase H activity facilitated reverse transcription. Finally, to test whether the observed termination frequencies may have been influenced by the method used to purify the RNA template, the GAG-3-primed polymerization time courses using gel-purified (+)-GAG^{345} were compared to those obtained using a cruder preparation of template that was purified by PhOH/$CHCl_3$ extraction of the transcription reaction, followed by ethanol precipitation. The pause-site frequencies were found to be largely unaffected by the method of purification with stalling of the mutants occurring in both cases with significantly higher frequency than the wild type at the RVI–RIX positions (data not shown). These data argued against the presence of a gel purification artifact which may have differentially affected the termination frequencies of the enzymes.

The effects of the RNase H mutations on the processivity of DNA synthesis directed by the RNA *gag* template were evaluated by comparing the products formed after the initiation of DNA synthesis by an E–hybrid complex in the presence of a large excess of challenger DNA. As shown in Figure 5, the similarity in the product distributions formed during a single processive cycle as opposed to unchallenged synthesis on the *gag* template suggested that all three enzymes processively reverse-transcribed the heteropolymer and that the processivity was limited by enzyme stalling at the high-frequency stop sites (lanes 2, 5, and 8 versus lanes 3, 6, and 9,

Table II: Steady-State Kinetic Parameters of the Wild-Type and Mutant Enzymes for DNA Polymerization of a Heteropolymer DNA·DNA Substrate[a]

enzyme	k_{cat} (s^{-1})[b]	K_M (nM)
wild type	0.12 ± 0.01	5.1 ± 0.6
D443N	0.10 ± 0.01	4.9 ± 1.5
D443N/D498N	0.07 ± 0.01	10.0 ± 5.0[c]

[a] RT filter assays were performed as described under Materials and Methods. At each subtrate concentration, initial rates were measured in duplicate from 0–5-min time courses. [b] Calculated on the basis of the total protein concentration. [c] Owing to the low polymerization rates (and hence sensitivity) in the low substrate concentration range (5–15 nM), this value is approximate.

respectively). The products formed during single processive cycles were quantitated by scanning densitometry, and the relative termination frequencies given in Figure 5 were calculated by the method of Abbotts et al. (1988).[2] All three enzymes terminated with different frequencies at preferred sites along the template, indicating a dependence of the termination frequency both on the RNase H phenotype [(+) versus (−)] and on the specific mutations. The wild-type enzyme terminated with high frequency at only 2 sites, after the addition of 7 (66%; RII) and 70 nt (95%; RXII), respectively. In contrast, the D443N mutant paused with highest frequency after the addition of 6 (12%; RI), 7 (33%; RII), 25 (5%), 26 (8%), 29 (26%; RVI), 31 (60%; RVIII), and 70 nt (95%; RXII), whereas the D443N/D498N mutant preferentially terminated after the incorporation of 6 (8%; RI), 7 (24%; RII), 29 (20%; RVI), 31 (66%; RVIII), and 70 nt (95%; RXII). Interestingly, no high-frequency termination was observed for any of the enzymes after the addition of 1–3 nt to the heteropolymer primer, in contrast to that observed for poly(A)-directed synthesis primed by dT_{12-14} (Figure 1; Majumdar et al., 1988).

DNA-Dependent DNA Synthesis. To investigate the effect of the chemical nature of the template on the DNA polymerization product distribution, the *gag* RNA template was replaced by a DNA template of identical sequence. As shown in Table II, the D443N mutation had a negligible effect on the steady-state kinetic parameters for replication of the ss-M13-ΔGAG-C/GAG-1 template-primer, whereas the double mutation lowered the k_{cat} 2-fold and increased the hybrid K_M ca. 2-fold. The gel electrophoretic time courses for synthesis by equimolar amounts of the three enzymes under multiple turnover conditions are shown in Figure 6. The product distributions for DNA-dependent synthesis were qualitatively and quantitatively similar for all three enzymes, indicating an insensitivity to the RNase H phenotype of the enzyme. In particular, the time courses of the wild-type and D443N mutant enzymes were almost identical with respect to the rate of DNA synthesis, and to the location of the pause sites (panel A vs B). Although the D443N/D498N time course showed accumulation of the same intermediate products, the product distribution was altered in a manner consistent with a slower rate of DNA synthesis relative to the other two enzymes (Table II). The positions and relative concentrations of the pause-site products formed under the multiple turnover conditions of Figure 6 are shown in Figure 7. In all cases, termination was observed after the addition of 1–7 nt (DI–DVI), after which stalling next occurred to give the major cluster of products DVIII–DX located a further 34–37 nt downstream of the primer terminus. A common feature of the majority of pause

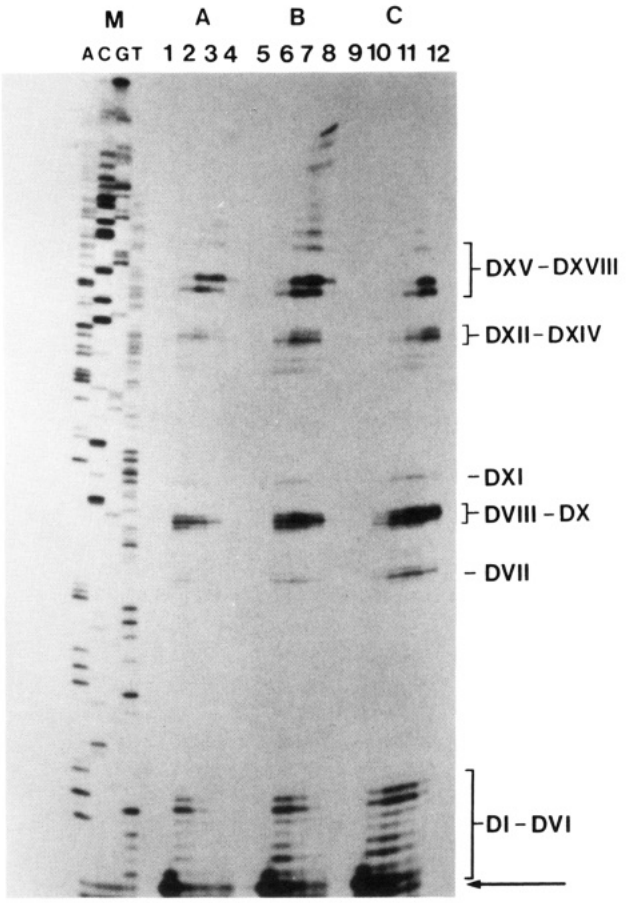

FIGURE 6: Heteropolymer DNA-dependent DNA polymerization. Time courses of RT-catalyzed DNA synthesis of ss-M13-ΔGAG-C/[5′-^{32}P]GAG-1 substrate catalyzed by wild-type (panel A), D443N (panel B), and D443N/D498N (panel C) enzymes. The dideoxy sequencing ladder (panel M) was used to determine the positions of the pause sites. Reactions containing 30 nM hybrid and 170 nM enzyme were incubated as described under Materials and Methods and were quenched and electrophoresed as described in the legend to Figure 3. The position of the unextended GAG-1 primer is indicated by an arrow. The termination products DI–DXVIII are referred to in the text.

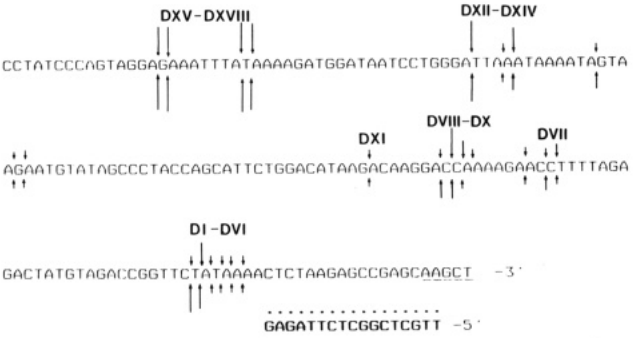

FIGURE 7: Pause sites of DNA synthesis on the *gag* DNA template. The locations of the pause sites DI–DXVIII (referred to in the text) within the *gag* insert region of the ss-M13-ΔGAG-C DNA template are indicated, as described in the legend to Figure 4. The arrow height represents the relative concentration of the product formed under the multiple turnover conditions of Figure 6.

[2] Relative termination frequencies were determined by measuring the ratio of products at the termination position versus products at that position plus all greater lengths. To be valid, this calculation requires that the extent of synthesis is restricted to prevent the further extension of initial pause-site products by multiple enzyme turnover, which would bias the frequencies in favor of larger products (Abbotts et al., 1988; Bebenek et al., 1989). This criterion was met by the conditions of the processivity assay, since the presence of the challenger DNA limited the polymerization to a single processive cycle by preventing significant reassociation of the enzyme to the hybrid substrate over the incubation period of the experiment (1–2 min).

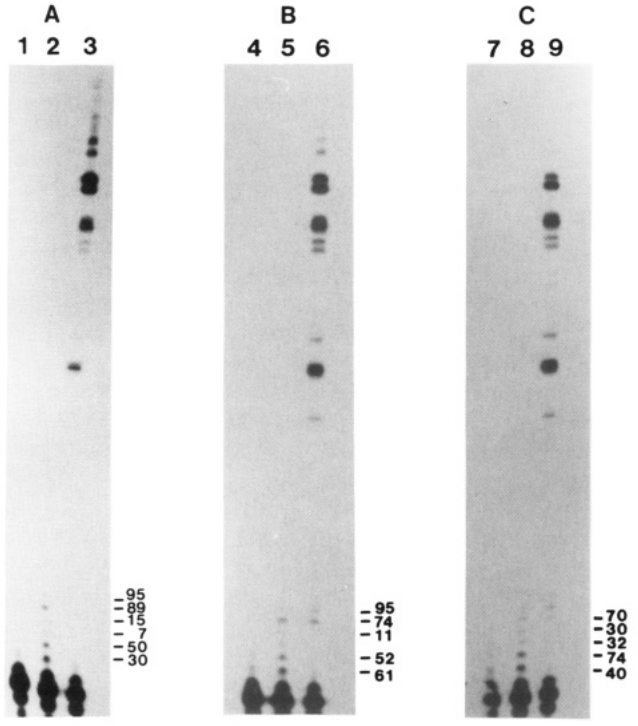

FIGURE 8: Processivity of DNA synthesis on a heteropolymer DNA template. (Panel A) Wild type; (panel B) D443N; (panel C) D443N/D498N. The substrate was ss-M13-ΔGAG-C/[5′-^{32}P]GAG1. Lane was as described in the legend to Figure 5. Final polymerization reactions containing 10 nM hybrid and either 50 nM (wild type) or 40 nM (mutant) RT enzyme were quenched after 2 min.

sites along the DNA template was their occurrence either within homopolymer stretches (DI–DIV) or immediately downstream of them (DV, DVI, DVII–DX, and DXII–DXVIII), in agreement with the reports of others (Bebenek et al., 1989; Huber et al., 1989; Hentosh et al., 1991).

As shown in Figure 8, the processivity of DNA-dependent DNA polymerization was very low for all three enzymes (lanes 2, 5, and 8). Since initial experiments conducted at the same final enzyme concentration as was used in the analogous RNA template experiments (Figure 5, 2 nM) resulted in no detectable processive synthesis, a 20-25-fold higher enzyme concentration was employed for the experiments of Figure 8.[3] The products of single processive cycles were compared to those of unchallenged synthesis (lanes 2, 5, and 8 versus lanes 3, 6, and 9, respectively). In all cases, the processivity was limited by the homopolymer tract in the template region 1–7 nt downstream of the primer at which high-frequency termination occurred.[2] In accordance with these results, Huber et al. (1989) reported a low processivity for the replication of poly(dA) by wild-type HIV-1 RT.

Discussion

The present study was aimed at analyzing the DNA polymerase activities of two point mutants of HIV-1 RT which specifically lacked RNase H activity. On the basis of the X-ray crystal structure of the RNase H domain of HIV-1 RT (Davies et al., 1991) and by analogy with the crystallographic data for the wild-type and mutant forms of the structurally related *E. coli* RNase H (Katayanagi et al., 1990; Yang et al., 1990), the structural consequences of the conserved aspartic acid to asparagine substitutions in the HIV-1 RT mutants used in this study were possibly limited to minor side-chain conformational changes within the RNase H domain alone. A homopolymer RNA template and related heteropolymer RNA and DNA templates containing regions of the same nucleotide sequence were employed to monitor the RNA- and DNA-dependent polymerase activities. A comparative kinetic analysis using the homopolymer substrate poly(A)·dT_{12-18} confirmed that the mutations had a negligible effect on the K_M and k_{cat} values of the enzyme. However, the ability of the RNase H mutants to reverse-transcribe a heteropolymer RNA template was noticeably impaired with respect to the extension of pause-site products. An analogous observation was alluded to by Kotewicz et al. (1988) for RNase H deletion mutants of Moloney murine leukemia virus RT but was not further discussed. The synthetic deficiency of HIV-1 RT was specific to heteropolymer RNA-dependent replication, since a comparison of the product distributions and kinetics of replication of a DNA version of the same template sequence showed no significant differences other than those attributable to a reduced k_{cat}/K_M value for the double-mutant enzyme.

The RNase H mutants retained the high processivity of reverse transcription of a poly(A) template that was characteristic of the wild-type enzyme (Majumdar et al., 1988; Huber et al., 1989), suggesting that the low frequency of termination along the polypurine template was largely unaffected by the RNase H phenotype of the enzyme. Similarly, the mutations hardly altered the processivity of DNA synthesis on a DNA heteropolymer, which was very low in all cases. In contrast, since the termination frequency at various positions along the RNA heteropolymer template was dependent on the RNase H phenotype of the enzyme, a smaller average product size was formed by the mutants compared to the wild type when synthesis was limited to a single processive cycle.

In terms of the kinetic model for polymerase processivity developed by Bryant et al. (1983), the processivity is determined by the k^{pol}/k^{off} ratio of the enzyme at successive template positions downstream of the initial primer terminus. The appearance of a prominent pause-site product is consistent with a low k^{pol}/k^{off} ratio at the corresponding template position which would result in the accumulation of an incompletely extended primer chain and, hence, limit the average product size formed during a single processive cycle. This ratio could be influenced by several factors, such as (i) the chemical nature of the template (RNA versus DNA), (ii) the structure of the duplex polymerization product (A for RNA-DNA, Z for DNA-DNA), (iii) the flanking nucleotide sequence, (iv) the size of the duplex product, and (v) the secondary structure of the template. A dependence on factors i and ii may explain the difference in the pause-site locations and processivity of HIV-1 RT on heteropolymer RNA and DNA templates of identical sequence, irrespective of the RNase H phenotype of the enzyme. The role of factor iii in pause-site and processivity determination on the *gag* DNA template was evident in the preferred location of the pause sites in the vicinity of homopolymer tracts, in agreement with the observations of others (Bebenek et al., 1989; Huber et al., 1989; Hentosh et al., 1991). The high-frequency termination of the RNase H mutants at the RVI–RIX positions was unaffected by replacing the GAG-1 primer by GAG-3, which primed synthesis a further 23 nt downstream (GAG-3) and thus argued against a dependence of pause-site location on the size of the duplex region 5′ to the primer terminus (factor iv). In contrast, although the preferred sites along two unrelated RNA heteropolymer templates did not correlate with specific template sequence [in agreement with the observations of Huber et al.

[3] As illustrated in lanes 1, 4, and 7 (Figure 8), the higher enzyme concentration lowered the efficiency of the DNA trap, resulting in a higher level of background incorporation.

(1989)], the clustering of pause sites within the loops of regions of potential RNA secondary structure suggested a degree of dependence on factor v. This conclusion was further supported by the lack of effect of the RNase H phenotype on the reverse transcription of poly(A), which is a template devoid of hairpinlike secondary structure. Comparative product distributions from reactions primed by the oligonucleotides GAG-1–GAG-3 suggested that changes in primer position that were relatively remote from prominent pause sites (>4 nt away) had a negligible effect on the termination frequencies of the enzymes. In contrast, changes in the relative termination frequencies were observed when the initial primer terminus was relocated to a position immediately adjacent to a prominent mutant enzyme pause site (RVI; replacement of GAG-1 by GAG-4). Since the hybridization of an oligonucleotide primer to the template potentially may alter the secondary structure of the RNA template beyond the primer terminus in a manner dependent on the specific location of the primer, a local structural change in the vicinity of RVI–RIX may have affected the pausing frequencies of the wild-type and mutant enzymes at these positions when synthesis was specifically primed by GAG-4.

The preliminary models of reverse transcription forwarded by several groups proposed a strict coupling of polymerase and ribonuclease activities, implying that the hybridized region 5′ to the primer terminus would remain approximately 15 base pairs long during RNA-dependent synthesis by the wild-type enzyme (Oyama et al., 1988; Schatz et al., 1990; Wöhrl & Moelling, 1990; Furfine & Reardon, 1991). However, during the course of this study, new evidence supporting an uncoupled mechanism was presented by DeStefano et al. (1991), suggesting that the duplex region 5′ to the primer terminus would become progressively longer during processive replication both by the wild-type and by the RNase H mutants.[4] Stalling of the wild-type enzyme at a natural pause site within a region of template secondary structure may facilitate conversion of the E–hybrid polymerase complex into an RNase H mode, which is otherwise kinetically disfavored during processive synthesis. The complex is thus poised for the obligate template cleavage step which precedes enzyme dissociation (DeStefano et al., 1991) and converts the hybrid into a form more amenable to further primer extension. In contrast, the inability of a RNase H mutant enzyme to hydrolyze the template may lock its conformation at a pause site in a polymerase mode disfavorable both to dissociation and to further DNA synthesis, thereby resulting in the accumulation of the pause-site product. A test of this hypothesis awaits further kinetic studies to identify the effect of the RNase H phenotype on the rates of the specific steps involved during single nucleotide incorporation. Finally, it should be stressed that although this model proposes a role for the RNase H activity in assisting the polymerase to traverse the template, certain blocks to reverse transcription by the wild-type enzyme nonetheless persist (e.g., RXII).

In conclusion, the results presented in this study have both theoretical and practical implications. First, since the mutations in the RNase H domain resulted in subtle alterations in the kinetics of polymerization on certain templates, the data support the notion of some degree of functional interplay between the polymerase and ribonuclease activities of the enzyme during reverse transcription. Second, with regard to the use of RT enzymes in molecular biology, Kotewicz et al. (1988) have outlined the advantages of RNase H RTs as tools for cDNA synthesis. Since the RNase H mutants of HIV-1 RT were impaired in their ability to generate a cDNA of a heteropolymer template, one obvious disadvantage to their use is the apparent difficulty to overcome the synthetic blocks presented by certain pause sites. Finally, Tisdale et al. (1991) recently showed that mutations in the COOH-terminal domain of HIV-1 RT which repressed the RNase H activity abolished viral infectivity, as had previously been observed for Moloney murine leukemia virus (Repaske et al., 1989). Although these data strongly implicated an essential role for the viral RNase H in determining infectivity, the results of our study suggested that minor changes in the RNA-dependent DNA polymerase activity disfavoring completion of (−)-strand DNA synthesis may also have contributed to the noninfectious phenotype of the RNase H domain mutants and further reinforce the therapeutic potential of viral RNase H inhibition.

[4] Since the product distributions illustrated in Figure 3 were obtained under conditions of an excess of enzyme over substrate, the excess wild-type enzyme, functioning exclusively as an RNase H, may have simultaneously degraded the RNA template during DNA synthesis. However, the wild-type product distributions formed under conditions of excess enzyme over substrate (multiple turnover; Figure 3, panel A, lanes 2–4) versus excess substrate over enzyme (one processive cycle; Figure 5, panel A, lane 2) were remarkably similar, suggesting either that insignificant cleavage by excess enzyme occurred during the time course of the experiment of Figure 3 or that concomitant template cleavage by RNase H enzyme did occur, but had no effect on the termination frequency of the polymerizing enzyme. These conclusions assume that in the presence of complementary dNTPs, under conditions in which [E] < [3′-OH], the enzyme functions exclusively as a polymerase rather than as a ribonuclease, which is justified on kinetic grounds (DeStefano et al., 1991).

Acknowledgments

We thank Professor Savage for use of the scanning densitometer and Mr. D. Beveridge, Mr. R. Brooksbank, and Mr. L. Teixeira for their invaluable assistance. We also thank Dr. J. Peliska and Mr. B. Eger for providing us with their modified T7 RNA polymerase purification procedure.

References

Abbotts, J., SenGupta, D. N., Zon, G., & Wilson, S. H. (1988) *J. Biol. Chem. 263*, 15094–15103.

Bebenek, K., Abbotts, J., Roberts, J. D., Wilson, S. H., & Kunkel, T. A. (1989) *J. Biol. Chem. 264*, 16948–16956.

Bryant, F. R., Johnson, K. A., & Benkovic, S. J. (1983) *Biochemistry 22*, 3537–3540.

Davies, J. F., II, Hostomska, Z., Hostomsky, Z., Jordan, S. R., & Matthews, D. A. (1991) *Science 252*, 88–95.

DeStefano, J. J., Buiser, R. G., Mallaber, L. M., Myers, T. W., Bambara, R. A., & Fay, P. J. (1991) *J. Biol. Chem. 266*, 7423–7431.

Dudding, L. R., Harington, A., & Mizrahi, V. (1990) *Biochem. Biophys. Res. Commun. 167*, 244–250.

Furfine, E. S., & Reardon, J. E. (1991) *J. Biol. Chem. 266*, 406–412.

Goff, S. P. (1990) *J. Acquired Immune Defic. Syndr. 3*, 817–831.

Grodberg, J., & Dunn, J. J. (1988) *J. Bacteriol. 170*, 1245–1253.

Hansen, J., Schulze, T., Mellert, W., & Moelling, K. (1988) *EMBO J. 7*, 239–243.

Hentosh, P., McCastlain, J. C., & Blakley, R. L. (1991) *Biochemistry 30*, 547–554.

Hizi, A., Hughes, S. H., & Shaharabany, M. (1990) *Virology 175*, 575–580.

Hostomsky, Z., Hostomska, Z., Hudson, G. O., Moomaw, E. W., & Nodes, B. R. (1991) *Proc. Natl. Acad. Sci. U.S.A. 88*, 1148–1152.

Huber, H. E., McCoy, J. M., Seehra, J. S., & Richardson, C. C. (1989) *J. Biol. Chem. 264*, 4669–4678.

Jacobo-Molina, A., & Arnold, E. (1991) *Biochemistry 30*, 6351–6361.
Joyce, C. M. (1989) *J. Biol. Chem. 264*, 10858–10866.
Katayanagi, K., Miyagawa, M., Matsushima, M., Ishikawa, M., Kanaya, S., Ikehara, M., Matsuzaki, T., & Morikawa, K. (1990) *Nature 347*, 306–309.
Kotewicz, M. L., Sampson, C. M., D'Alessio, J. M., & Gerard, G. F. (1988) *Nucleic Acids Res. 16*, 265–277.
Majumdar, C., Abbotts, J., Broder, S., & Wilson, S. H. (1988) *J. Biol. Chem. 263*, 15657–15665.
Mizrahi, V. (1989) *Biochemistry 28*, 9088–9094.
Mizrahi, V., Benkovic, P. A., & Benkovic, S. J. (1986) *Proc. Natl. Acad. Sci. U.S.A. 83*, 5769–5773.
Mizrahi, V., Lazarus, G. M., Miles, L. M., Meyers, C. A., & Debouck, C. (1989) *Arch. Biochem. Biophys. 273*, 347–358.
Mizrahi, V., Usdin, M. T., Harington, A., & Dudding, L. R. (1990) *Nucleic Acids Res. 18*, 5359–5363.
Oyama, F., Kikuchi, R., Crouch, R. J., & Uchida, T. (1989) *J. Biol. Chem. 264*, 18808–18817.
Panganiban, A. T., & Fiore, D. (1988) *Science 241*, 1064–1069.
Prasad, V. R., & Goff, S. P. (1989) *Proc. Natl. Acad. Sci. U.S.A. 86*, 3104–3108.
Repaske, R., Hartley, J. W., Kavlick, M. F., O'Neill, R. R., & Austin, J. B. (1989) *J. Virol. 63*, 1460–1464.
Schatz, O., Cromme, F. V., Grüninger-Leitch, F., & Le Grice, S. F. J. (1989) *FEBS Lett. 257*, 311–314.
Schatz, O., Mous, J., & Le Grice, S. F. J. (1990) *EMBO J. 9*, 1171–1176.
Tan, C.-K., Zhang, J., Li, Z.-Y., Tarpley, W. G., Downey, K. M., & So, A. G. (1991) *Biochemistry 30*, 2651–2655.
Tanese, N., & Goff, S. P. (1988) *Proc. Natl. Acad. Sci. U.S.A. 85*, 1777–1781.
Tisdale, M., Schulze, T., Larder, B. A., & Moelling, K. (1991) *J. Gen. Virol. 72*, 59–66.
Wöhrl, B. M., & Moelling, K. (1990) *Biochemistry 29*, 10141–10147.
Yang, W., Hendrickson, W. A., Crouch, R. J., & Satow, Y. (1990) *Science 249*, 1398–1405.

Vitamin K Dependent Carboxylation: Determination of the Stereochemical Course Using 4-Fluoroglutamyl-Containing Substrate†

Joëlle Dubois,‡,§ Christophe Dugave,§ Christine Fourès,§ Marthe Kaminsky,§ Jean-Claude Tabet,‖ Sonia Bory,§ Michel Gaudry,*,§ and Andrée Marquet§

Laboratoire de Chimie Organique Biologique, URA CNRS 493, Université Pierre et Marie Curie, 4, place Jussieu, 75252 Paris Cedex 05, France, and Laboratoire de Chimie Organique Structurale, URA CNRS 455, Université Pierre et Marie Curie, 4, place Jussieu, 75252 Paris Cedex 05, France

Received April 9, 1991; Revised Manuscript Received July 24, 1991

ABSTRACT: The stereochemical course of the vitamin K dependent carboxylation has been elucidated using a (4*S*)-4-fluoroglutamyl-containing pentapeptide as a substrate. The absolute configuration of the [^{13}C]-4-carboxy-4-fluoroglutamate obtained when the carboxylation was carried out with ^{13}C-labeled sodium bicarbonate, was determined after reduction of the [^{13}C]-4-carboxy-4-fluoroglutamyl residue into 4-fluoro-5,5′-dihydroxyleucine, hydrolysis, lactonization, and peracetylation. The absolute configuration at C-4 was determined to be *S* by locating the ^{13}C label in the lactone ring of the trans isomeric lactone and in the hydroxymethyl group of the cis isomer following HPLC separation of both isomers and analysis by GC/MS/MS techniques. It follows that the vitamin K dependent carboxylation occurs with inversion of configuration.

Vitamin K is the cofactor of the posttranscriptional carboxylation of glutamic residues into 4-carboxyglutamic residues which are present in blood coagulation factors, in some bone proteins, and in mineralized tissues (Suttie, 1980, 1985, 1988).

Early studies with *threo*- and *erythro*-4-fluoroglutamate-containing substrates (Dubois et al., 1983) and isotope effect determinations (Decottignies et al., 1984a,b) established that the carboxylase selectively abstracts the 4-*proS* hydrogen (Scheme I).

Scheme I: Possible Stereochemical Course of Vitamin K Dependent Carboxylation of Glutamyl Residues

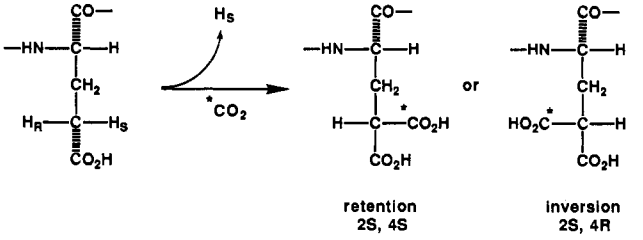

In order to elucidate the stereochemistry of the reaction, it was necessary to determine the absolute configuration of the 4-carboxyglutamate obtained when ^{14}C- or ^{13}C-labeled carbon dioxide is used: a 4*R* configuration will correspond to an inversion of configuration and vice versa (Scheme I).

† This research was supported by the Centre National de la Recherche Scientifique and the Université Pierre et Marie Curie.
‡ Present address: Institut de Chimie des Substances Naturelles, CNRS, 91190 Gif-sur-Yvette, France.
§ Laboratoire de Chimie Organique Biologique.
‖ Laboratorie de Chimie Organique Structurale.

0006-2960/91/0430-10506$02.50/0